Journal of Engineering and Sustainable Development
http://jeasd.uomustansiriyah.edu.iq/index.php
https://doi.org/10.31272/jeasd.26.3.2

JEASD

Vol. 26, No. 03, May 2022
ISSN 2520-0917

NUMERICAL INVESTIGATION OF A MANTLE HEAT EXCHANGER

***Amina M. Ogla** **Aouf A. Al-Tabbakh**

Mechanical Engineering Department, College of Engineering, Mustansiriyah University, Baghdad, Iraq

Received 13/10/2021 ***Accepted in revised form 18/11/2021*** ***Published 1/5/2022***

Abstract: The following work deals with numerical investigation of a storage tank equipped with a mantle annular cavity surrounding it. Heat is transferred via the working fluid flowing in the mantle side to the inner storage tank. Water at constant temperature of 60 oC enters the mantle to heat the tank and exits at a lower temperature. The study is carried out using the commercial software Ansys−Fluent to track the change of water temperature in the tank and mantle side during the simulated period of 60 minutes. Temperature contours of tank water and mantle water are drawn at several time intervals during the simulated period. The effects of changing working fluid mass flow rate were taken into account through three values, namely; 0.0077, 0.015 and 0.02 kg/s. Three values of mantle gap thickness; 10, 15 and 20 mm, and three values of mantle length; 250, 300 and 350 mm were applied in the simulation program and their effects were monitored and displayed. Results show that increasing the value of mass flow rate causes more heat transfer rate to the storage tank. The gap thickness of 10 mm which is the smallest value among the three applied values gave the best heat transfer rate and the mantle length of 300 mm was the optimum among the applied values. The heat transfer rate to the tank was studied in terms of tank mean temperature. The maximum mean tank temperature achieved at the end of the simulated period was 42 oC.

Keywords: *mantle heat exchanger*, *storage tank*, *CFD modeling*, *temperature contours*

1. Introduction

Mantle heat exchangers or mantled storage tanks are usually employed in the field of solar energy engineering as a means of heat transfer between the solar collector working fluid and the storage medium. The importance of using mantle heat exchangers are the efficient heat transfer between the working fluid and the storage tank, freeze protection inside the solar collector that is connected to the mantle and the simplification in design and mounting because the heat exchanger and tank becomes a single unit (S. Furbo, 1992) [1]. A typical mantle heat exchanger consists of a conventional water storage tank wrapped from outside by an annular cavity or (mantle) through which the working fluid flows. The area of heat transfer is greatly increased by this configuration and the frictional losses are decreased. Thermal stratification inside the tank may also be enhanced especially in vertical orientation of the storage tank. The research work in mantle Heat exchangers started at the early nineties by the works of (S. Furbo, 1992) [1], (S. Furbo and P. Berg, 1992) [2] and (S. Furbo, 1992) [3]. The

**Corresponding Author*: aminamh15@gmail.com

researches focused on transient modeling using finite differences. Another approach was adopted by (J. M. Baur et al., 1993) [4], by dividing the storage tank into several horizontal layers. The water at each layer was assumed fully mixed with radial temperature ignored. Detailed CFD modeling on a vertical mantled tank was conducted by (L. J. Shah and S. Furbo, 1998) [5]. The water flow rate employed was comparable in value to that applicable in solar water heaters. Three dimensional body fitted technique was applied to the tank domain with 42, 25 and 10 nodes in axial, radial and circumferential directions respectively. Buoyancy effects were modeled using Boussinesq approximation. The theoretical results were also experimentally validated. Visualization techniques were also used to monitor and understand the flow patterns of working fluid in the tank and mantle sides. (L. J. Shah et al., 1999) [6] applied Particle Image Velocimetry PIV technique on a rectangular mantle storage tank. The results obtained from the rectangular device approaches the results of circular device for small mantle gap/tank diameters ratios. The effects of using mantle heat exchanger on the yearly performance of a solar water heater was investigated by (L. J. Shah, 2001) [7]. CFD results were combined with empirical correlations describing the long term performance of the system. Various values mantle gap thickness, tank height to diameter ratio and mass flow rate were used in the correlations. The results were compared with actual measurements of temperature and heat flux and good agreement was achieved. The effect of using mantle heat exchanger on thermal stratification was further studied experimentally and numerically by (S. Knudsen and S. Furbo, 2004) [8]. A Ph.D. thesis (S. Knudsen, 2004) [9] was entirely devoted to study and analyze a low flow rate solar domestic water heater containing mantle heat exchanger. (S. Knudsen, G. L. Morrison, 2005) [10] performed a visualization study on the mantle and tank sides via PID method. The initial condition of the tank was assumed fully mixed once and thermally stratified once again. The effect of a variable inlet port temperature was also considered.

Previous research work on mantle heat exchangers included most of the relevant design and performance parameters. However, detailed studies regarding the temperature distributions in both mantle and tank sides are still required. The aim of the present work is to numerically analyze the thermal performance of a vertical mantle heat exchanger. The study will employ the commercial software Ansys Fluent to estimate the temperature and velocity distributions on both mantle and tank sides. The theoretical results will be compared with experimental measurements for the sake of validation. The effect of some design and performance parameters will also be studied.

2. Numerical Computation

The problem at hand is a three-dimensional transient heat transfer between the working fluid flowing at a constant inlet velocity in the mantle and the stagnant water in the tank via the metal interface between the mantle and tank. To solve the problem and estimate the transient velocity and temperature distributions in both the mantle and tank sides, the commercial CFD software Ansys Fluent is used. The simulation procedure is divided into the following steps:

a- The geometrical model is created by the (Design Modeler)
b- Discretizing the mantle and tank domains through the (Mesh Platform)
c- Resolving the issue by (Fluent 16.2 CFD solver)

2.1. Geometric Modeling

The current system's geometries are drawn using Ansys Design Modeler. The first step in numerical simulation is to define the geometry. It entails drawing a cylindrical tank surrounded by a mantle, with inlet and outlet ports on both the mantle and tank sides, as shown in (Fig. 1). The system's dimensions are given in (table 1). Water, stainless steel, and glass wool properties are given in (table 2).

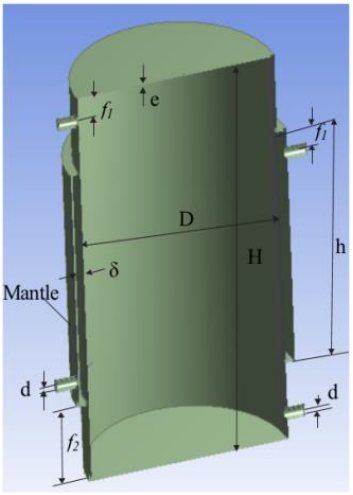

Figure 1. A cross-section of the mantle heat exchanger.

Table 1. Mantle heat exchanger specifications.

Tank inner height (H), [mm]	500
Mantle inner height (h), [mm]	250,300,350
Tank inner diameter (D), [mm]	250
Tank wall thickness (e), [mm]	2
Insulation material	Glass Wool
Insulation thickness, [mm]	0.025
Inlet and outlet ports diameter (d), [mm]	10
Mantle gap thickness (δ), [mm]	10,15,20
Distance from tank roof/base to tank inlet/outlet port (f_1) [mm]	25
Distance from tank roof/base to mantle edge (f_2) [mm]	100
Mantle-tank interface area (A_s), [m^2]	0.2379
Tank volume (V), [m^3]	0.02452

Table 2. Material characteristics

Water Properties	
Specific Heat [J/Kg.K]	4182
Density [Kg/m^3]	998.2
Thermal Conductivity [W/m.K]	0.6
Viscosity [Kg/m.s]	0.001003
Stainless Steel Properties	
Specific Heat [J/Kg.K]	460
Density [Kg/m^3]	7820
Thermal Conductivity [W/m.K]	15
Glass Wool Properties	
Specific Heat [J/Kg.K]	840
Density [Kg/m^3]	20
Thermal Conductivity [W/m.K]	0.03

2.2. Mesh Generation

The temperature distributions in the tank and mantle sides are evaluated by discretizing the two domains into tiny elements. The entire computational domain is transformed into a mesh like grid with a massive number of elements. The tank and mantle domains were analyzed and discretized as computational domains. The mesh generation process is carried out by the CFD software Ansys 16.2 to generate 255,609 elements in both domains. (Fig. 2) depicts the discretized mantle heat exchanger.

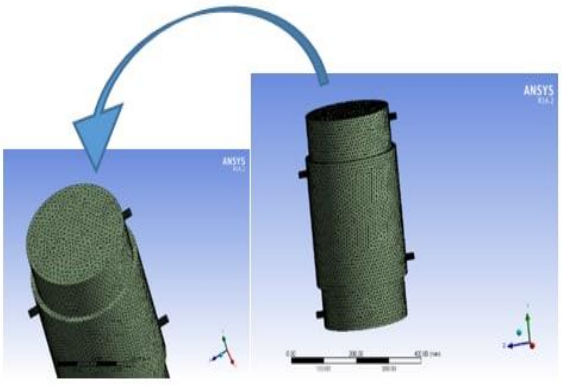

Figure 2. Discretized mantle heat exchanger.

2.3. Boundary Conditions

In the computational model, three types of boundary conditions were used:

1. Inlet boundary condition: the mantle inlet temperature is 60 °C. In both modes, the mantle inlet velocity is 0.1 m/s and the velocity in the tank is zero.
2. Initial condition: The tank is initially assumed to be at 20 °C.
3. Wall boundary condition: The velocity at any solid surface is assumed to be zero (no slip condition).

2.4. Boundary Conditions

The thermal problem in the mantle heat exchanger is analyzed using continuity, momentum, and energy equations in three dimensions. The transient case will be examined to determine how temperature profiles change over time. Depending on the definitions of $\boldsymbol{\phi}$, $\boldsymbol{\Gamma_\phi}$ and $\mathbf{S_\phi}$ in (table 3) [11], the following general equation (1) can be used to form the three conservation laws.

$$\frac{\partial \phi}{\partial t}+\frac{1}{r}\frac{\partial r V_r \phi}{\partial r}+\frac{1}{r}\frac{\partial V_\theta \phi}{\partial \theta}+\frac{\partial V_z \phi}{\partial z}=\Gamma_\phi\left[\frac{1}{r}\frac{\partial}{\partial r}\left(r\frac{\partial \phi}{\partial r}\right)+\frac{1}{r^2}\frac{\partial^2 \phi}{\partial \theta^2}+\frac{\partial^2 \phi}{\partial z^2}\right]+S_\phi \quad (1)$$

Where denotes a general variable that can represent the physical quantity under consideration per unit mass. The symbols Vr, V, and Vz represent the r, v, and z velocity components, respectively. The remaining symbols ρ, Γ_ϕ and S_ϕ, represent the density, diffusion coefficient, and source term corresponding to ϕ, respectively.

Table 3. The expressions for the parameters ϕ, Γϕ and Sϕ for the 3-D cylindrical coordinate system.

Equation	$\boldsymbol{\phi}$	$\boldsymbol{\Gamma_\phi}$	$\mathbf{S_\phi}$
Continuity	1	0	0
Momentum in r direction	V_r	v	$\frac{1}{\rho}\frac{\partial P}{\partial r}+g_r\frac{(\rho-\rho_\infty)}{\rho}+\frac{V_\theta^2}{r}-v\frac{2}{r^2}\frac{\partial V_\theta}{\partial \theta}-v\frac{V_r}{r^2}$
Momentum in θ direction	V_θ	v	$\frac{1}{\rho r}\frac{\partial P}{\partial \theta}+g_\theta\frac{(\rho-\rho_\infty)}{\rho}+\frac{V_r V_\theta}{r}-v\frac{2}{r^2}\frac{\partial V_r}{\partial \theta}-v\frac{V_\theta}{r^2}$
Momentum in z direction	V_z	v	$-\frac{1}{\rho}\frac{\partial P}{\partial z}+g_z\frac{(\rho-\rho_\infty)}{\rho}$
Energy	T	$\frac{k}{\rho c_p}$	$\frac{\Phi_d}{\rho c_p}$

WhereΦ_d is the viscous dissipation function denoted by the equation:

$$\Phi_d=2\mu\left(\frac{\partial V_r}{\partial r}\right)^2+\frac{2\mu}{r^2}\left(\frac{\partial V_\theta}{\partial \theta}+V_r\right)^2+2\mu\left(\frac{\partial V_z}{\partial z}\right)^2+\mu\left(\frac{\partial V_\theta}{\partial z}+\frac{1}{r}\frac{\partial V_z}{\partial \theta}\right)^2+\mu\left(\frac{\partial V_\theta}{\partial r}+\frac{\partial V_r}{\partial z}\right)^2+\mu\left[\frac{1}{r}\frac{\partial V_r}{\partial \theta}+r\frac{\partial}{\partial \theta}\left(\frac{V_\theta}{r}\right)\right]^2+G_e \quad (2)$$

3. Results and Discussion

The simulations are designed to investigate the system's transient thermal performance as a result of various operating conditions and geometrical parameters. The simulations were run at different time intervals ranging from 300 to 3600 seconds. The simulations used three different mass flow rate values. The effects of changing the mantle gap thickness and length were also taken into account. The sequence of variation of mantle and tank temperature contours for selected time intervals between 0 and 3600 s for a mass flow rate of 0.0077 kg/s, mantle gap of 10 mm, and mantle length of 300 s is shown in Fig. 3. Fig. 4 show the effects of increasing the mass flow rate to 0.0077, 0.015 and 0.02 kg/s, respectively. Increasing the mass flow rate has a clear effect on increasing the

tank's heating rate and accelerating heat penetration. Fig .5 show temperature contours for mantle gaps of 10, 15 and 20 mm, respectively. Increasing the value of the mantle gap results in a slower heating rate and less thermal energy penetration in the tank water. The increased length of the mantle provides more heat transfer area and better heat penetration in the tank water.

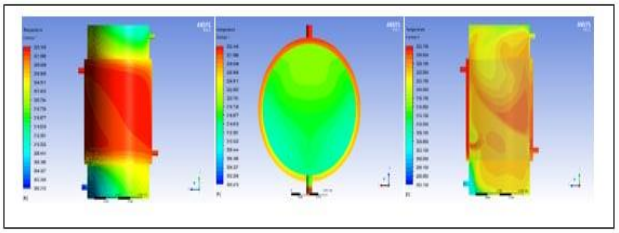

Figure 3. Temperatures contours of the tank (right and middle) and mantle (left) at ṁ= 0.0077 kg/s, mantle gap of 10 mm and mantle length of 300 mm at 3600s.

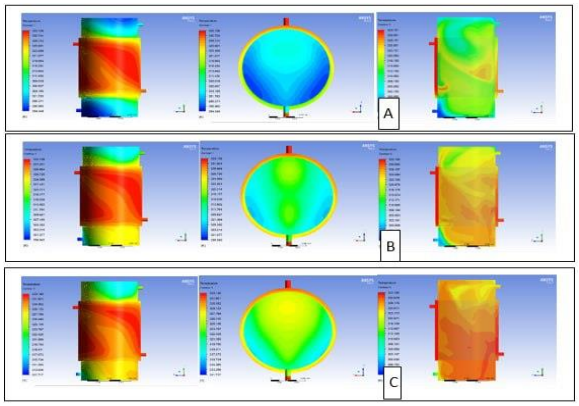

Figure 4. Temperatures contours of the tank (right and middle) and mantle (left) at mantle gap of 10 mm and mantle length of 300 mm for mass flow rate: (A)ṁ= 0.0077 kg/s, (B) ṁ= 0.015 kg/s, (C) ṁ= 0.02 kg/s, at 1800s.

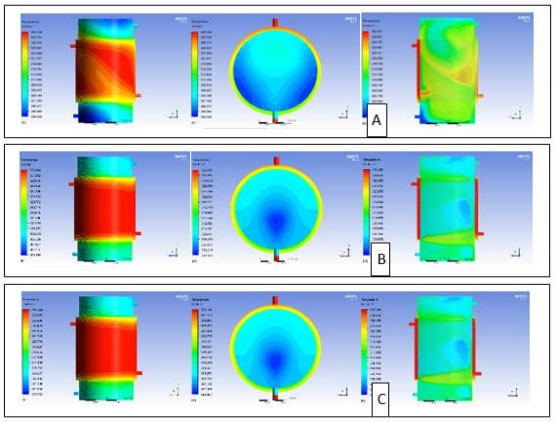

Figure 5. Temperatures contours of the tank (right and middle) and mantle (left) at ṁ= 0.0077 kg/s and mantle length of 300 mm for mantle gap of: (A)10mm, (B) 15mm, (C) 20mm, at 1800s.

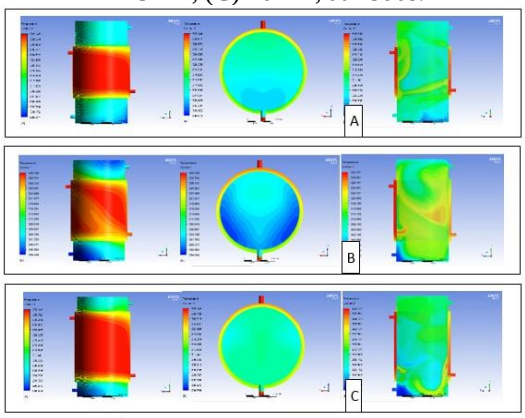

Figure 6. Temperatures contours of the tank (right and middle) and mantle (left) at ṁ= 0.0077 kg/s, mantle gap of 10 mm, mantle length of: (A) 250mm, (B) 300mm, (C) 350mm, at 1800s.

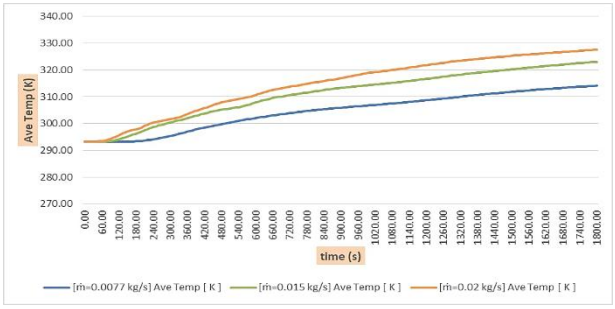

Figure 7. Variation of tank average temperature with time for three values of ṁ= 0.0077, ṁ= 0.015 and ṁ= 0.02 kg/s.

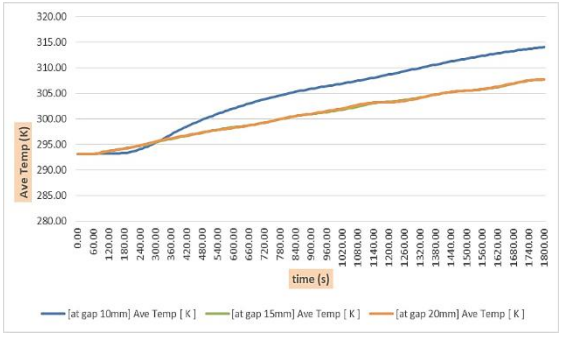

Figure 8. Variation of tank average temperature with time for three values of mantle gap: 10, 15 and 20mm.

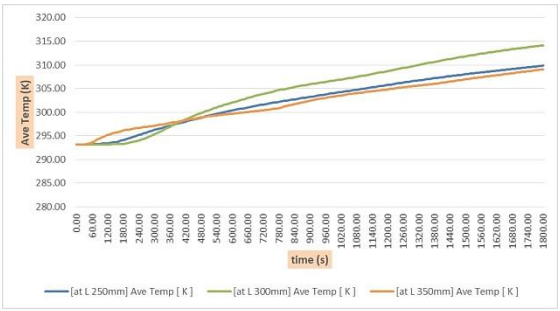

Figure 9. Variation of tank average temperature with time for three values of mantle length: 250, 300 and 350mm.

4. Comparison With other Works

The numerical results of the present work were compared with the results of Arslan and Igci [11] and the comparisons are shown in Figs. 10 and 11. The first figure displays tank average temperature versus time while the second figure is plotted in terms of a non−dimensional temperature versus a non−dimensional time. The non−dimensional temperature is defined by the following equation:

$$T^* = \frac{T_{avg} - T_{min}}{T_{min} - T_{max}} \qquad (3)$$

Where T_{avg} is the tank average temperature and T_{min} and T_{max} are the minimum and maximum temperatures throughout the tank at the moment of time under consideration, respectively. The non−dimensional time is define as the time under consideration divided by the total simulation time.

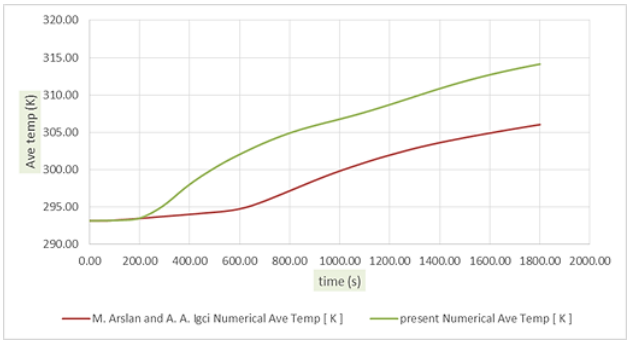

Figure 10. Comparison between the current simulation results with the results of Arslan and Igci [11]. Temperature vs. time.

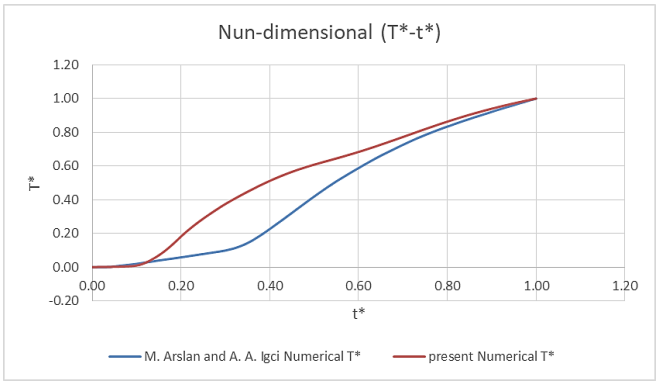

Figure 11. Comparison between the current simulation results with the results of Arslan and Igci [11]. Non−dimensional temperature vs. non−dimensional time.

5. Conclusions

The present work is a numerical and experimental study of a mantle heat exchanger. Thermal performance in the transient phase is estimated by a simulation procedure using the commercial CFD software Ansys−Fluent. The following conclusions can be drawn from the present study:

1. Increasing the value mass flow rate broadens and accelerates heat penetration in the tank. With increasing mantle mass flow rate, the heat transfer rate to the tank increases.
2. Changing the geometrical parameters (mantle gap and mantle length) had similar effects to the cooling mode, but in the opposite direction.
3. For a tank volume of 0.024 m3 initially at 20 °C, the time required to reach steady state is slightly. The final tank temperature averaged 50 °C.

Acknowledgements

I wish to acknowledge and appreciate the support given by the Faculty of Engineering at Al-Mustansiriyah University to successfully accomplish the theoretical and experimental phases of this research.

Conflict of interest

The authors confirm that the publication of this article causes no conflict of interest.

Abbreviations

As	*Heat transfer surface area between mantle and tank, m2*
d	Inlet and exit diameter of tank and mantle, m
D	Tank internal diameter, m
e	Tank wall thickness, m
C_p	Specific heat, J/kg.K
f1	Inlet and outlet distance to top/bottom of tank and mantle, m
f2	Height of the mantle to bottom of the tank, m
g	Gravitational acceleration, m/s2
Ge	Energy generation rate per unit volume, W
h	Total height of inner mantle, m
H	Tank height, m
k	Number of time interval
k	Thermal conductivity of the water, W/m.K
r	Radial distance, m
R	Radius, m
t	Time, s
ṁ	Mass flow rate , Kg/s
T	Temperature, K
V	Inner tank volume, m3
Vr	Radial direction velocity component, m/s
Vθ	Angular direction velocity component, m/s
Vz	Axial direction velocity component, m/s
z	Axial distance, m

6. References

1. S. Furbo, “Solar water heating systems using low flow rates - experimental investigations,” Thermal Insulation Laboratory, Technical University of Denmark, 1992.
2. S. Furbo and P. Berg, “Calculation of the thermal Performance of small hot water solar heating systems using low flow operation,” Thermal Insulation Laboratory, Technical University of Denmark, 1992.
3. S. Furbo, “PC model for low flow solar heating systems,” Thermal Insulation Laboratory, Technical University of Denmark, 1992.
4. J. M. Baur, S. A. Klein, and W. A. Beckman, “Simulation of water tanks with mantle heat exchangers,” in *The 1993 Americal Solar Energy Society Annual Conference*, 1993.
5. L. J. Shah and S. Furbo, “Correlation of experimental and theoretical heat transfer in mantle tanks used in low flow SDHW systems,” *Sol. Energy*, vol. 64, no. 4–6, pp. 245–256, 1998, doi: 10.1016/S0038-092X(98)00093-0.
6. L. J. Shah, G. L. Morrison, and M. Behnia, “Characteristics of vertical mantle heat exchangers for solar water heaters,” *Sol. Energy*, vol. 67, no. 1–3, pp. 79–91, 1999, doi: 10.1016/S0038-092X(00)00044-X.
7. L. J. Shah, “Heat transfer correlations for vertical mantle heat exchangers,” *Sol. Energy*, vol. 69, no. SUPPLEMENT, pp. 157–171, 2001, doi: 10.1016/S0038-092X(01)00039-1.
8. S. Knudsen and S. Furbo, “Thermal stratification in vertical mantle heat-exchangers with application to solar domestic hot-water systems,” *Appl. Energy*, vol. 78, no. 3, pp. 257–272, 2004, doi: 10.1016/j.apenergy.2003.09.002.
9. S. Knudsen, “Investigation and optimisation of heat storage tanks for low-flow SDHW systems,” Ph.D. Thesis, Technical University of Denmark, 2004.
10. S. Knudsen, G. L. Morrison, M. Behnia, and S. Furbo, “Analysis of the flow structure and heat transfer in a vertical mantle heat exchanger,” *Sol. Energy*, vol. 78, no. 2, pp. 281–289, 2005, doi: 10.1016/j.solener.2004.08.019.

11. M. Arslan and A. A. Igci, “Thermal performance of a vertical solar hot water storage tank with a mantle heat exchanger depending on the discharging operation parameters,” *Sol. Energy*, vol. 116, pp. 184–204, 2015, doi: 10.1016/j.solener.2015.03.045.
12. G. Rao, K. Reddy, and M. Reddy, “Influencing parameters on performance of a mantle heat exchanger for a solar water heater - a simulation study,” Int. J. Eng. Sci. Technol., vol. 2, no. 2, pp. 155–164, 2010, doi: 10.4314/ijest.v2i2.59160.
13. M. Arslan and A. A. Igci, “Thermal performance of a vertical solar hot water storage tank with a mantle heat exchanger depending on the discharging operation parameters,” Sol. Energy, vol. 116, pp. 184–204, 2015, doi: 10.1016/j.solener.2015.03.045.
14. D. Erdemir and N. Altuntop, “Improved thermal stratification with obstacles placed inside the vertical mantled hot water tanks,” Appl. Therm. Eng., vol. 100, pp. 20–29, 2016, doi: 10.1016/j.applthermaleng.2016.01.069.